Acta Cryst. (1973). A**29**, 283

On the Effect of Limited Instrumental Resolution on the TDS Correction of Bragg Reflexions

BY C. SCHERINGER

Institut für Kristallographie der Universität, Karlsruhe, Germany (BRD)

(*Received* 30 *October* 1972; *accepted* 20 *November* 1972)

If the TDS correction of Bragg reflexions is evaluated by integrating the TDS interference function over the range of measurement, the correction is usually, as Cochran has pointed out, too large. The magnitude of the 'overcorrection' is difficult to estimate since the proper evaluation of the correction involves the convolution of the interference function with the resolution function of the experimental set-up. Thus, in general, a sixfold integration is involved. Here calculations performed with a simple model which contains the essential features of the problem, and for which the integrations can be carried out properly, are reported. It has been found that the size of the 'overcorrection' depends only a little upon the absolute size of the range of measurement but strongly upon the size of the range of measurement relative to the magnitude of instrumental broadening (Bragg peak). With decreasing range of measurement relative to the Bragg peak the 'overcorrection' increases rapidly. For typical experimental situations of single-crystal measurements the 'overcorrection' seems to amount to about 5 to 20% of the TDS correction.

1. Introduction

If one wants to determine the intensity of the Bragg reflexions most accurately the thermal diffuse scattering (TDS), which has sharp maxima at the reciprocal-lattice points, has to be subtracted from the intensity measured at the reciprocal-lattice points. This 'TDS correction' has usually been evaluated in the past by integrating the TDS interference function over the range of measurement of the Bragg peak. Cochran (1969) pointed out that this procedure suffers from one main deficiency: through some instrumental factors (divergence of primary beam, finite crystal size, mosaic spread, wavelength distribution) the intensity profile is broadened so that the peak of this profile at the reciprocal-lattice points is less sharp than that of the interference function. The proper evaluation of the TDS correction demands the integration of the actual profile over the range of measurement, and this will, in general, result in a smaller value of the correction, *cf.* Cochran (1969). The integration over the interference function thus leads to an 'overcorrection' which may contain larger errors than those which one wanted to eliminate in the past by making more accurate assumptions concerning the form of the range of measurement and the anisotropy of the TDS interference function.

In actual practice the accurate development of Cochran's proposals involves great difficulties. In evaluating the correction the convolution of the TDS interference function with the three-dimensional resolution function is involved, and this amounts to a sixfold integration. In general, this integration can be performed neither analytically nor numerically. Furthermore, the actual resolution functions for a given experimental set-up are usually not precisely known. One way out is proposed by Walker & Chipman (1970), and Jennings (1970) in that they treat the effects of instrumental broadening one-dimensionally (in the direction of scan) and try to eliminate them in the two other directions by opening wide the detection window.

In order to gain insight into the magnitude of the effect of three-dimensional instrumental broadening we want to treat the problem three-dimensionally. Of course, this can only be done by assuming a simple model with respect to interference and resolution functions. The model which we use does not strictly correspond to normal experimental situations but it contains the essential features of the problem and can be treated mathematically. In the following we first describe the TDS interference and resolution functions which we use. Then we consider the resulting convolution integrals and their solutions. They provide the actual TDS correction. A factor R is defined, with $0<R\leq 1$, which formally describes the effect of limited instrumental resolution on that TDS correction which is obtained by using only the interference function ($R=1$ holds for the ideal case of unlimited resolution). Numerical results are computed and will be discussed.

2. Interference and resolution functions

In this paper we use the spherical–symmetrical approximation

$$I_1(r)=\frac{C}{r^2} \tag{2.1}$$

for the TDS interference function. r is the distance of a reference point to the reciprocal-lattice point under consideration, expressed in units of a cubic reciprocal lattice. C is a constant. The approximation (2.1) corresponds to choosing the first order of the acoustic spectrum with a mean elastic constant, *cf.* Nilsson (1957), Cooper & Rouse (1968) and Cochran (1969). According to Cochran (1969) only the first order of the acoustic TDS spectrum matters; neither the higher

orders nor the optic modes give relevant contributions. As Skelton & Katz (1969) have shown with an example, the use of a spherical interference function of type (2.1) gives rise to an error of less than 5% of the correction. The constant C in equation (2.1) only contains physical constants, the lattice constant of the cubic crystal, and the magnitude of the reciprocal-lattice vector considered, *cf.* Cochran (1969, equation 3.4).

Equation (2.1) is not quite accurate for finite crystals: $I_1(r)$ becomes infinitely large for $r=0$. This is physically meaningless and also causes trouble in the final numerical integration, which we shall encounter below. An upper limit of $I_1(r)$ for finite crystals can be obtained as follows. Let the crystal have N_1 cells in each direction of space: then, by using the cyclic boundary condition, the largest wavelength in the crystal is $\lambda_{max}=N_1 a$, and the respective interference maximum is located at a distance of $\lambda_{max}^{-1}=N_1{}^{-1}$ a Å^{-1} from the reciprocal-lattice point considered, *cf.* James (1948, p. 202). Instead of equation (2.1) we now may write, to a fully sufficient approximation,

$$I_1(r)=\frac{C}{r^2+N_1{}^{-2}}\,. \tag{2.2}$$

For $r=0$ we now have $I_1=N_1^2$, and the singularity is thus removed.

In order to simulate instrumental broadening, Gaussian resolution functions will be used. Gaussian functions are probably best suited to express actual profiles, and they have the advantage of converging rapidly to zero. We introduce orthogonal coordinates xyz and $x'y'z'$ in reciprocal space, scale them in reciprocal-lattice units, and refer them to the reciprocal-lattice point considered. Then, for three, two, and one-dimensional instrumental broadening, we use the functions

$$G(xyz)=(a/\pi)^{3/2}\exp[-a(x^2+y^2+z^2)]\,, \tag{2.3}$$

$$G(xy)=\frac{a}{\pi}\exp\,[-a(x^2+y^2)]\,, \tag{2.4}$$

$$G(z)=(a/\pi)^{1/2}\exp\,(-az^2) \tag{2.5}$$

respectively. All functions are normalized, *i.e.* their integrals from $-\infty$ to $+\infty$ are unity. It would, of course, be better to use a normalized Gaussian function with three parameters according to $\sqrt{\frac{abc}{\pi}^3}\exp\{-(ax^2+by^2+cz^2)\}$ but then the convolution integrals cannot be solved. However, our three special functions still give a representative survey since, in actual practice, the background is not measured at a single point but is rather averaged over a certain area in reciprocal space, *cf.* Cochran (1969). Therefore the effect of the extreme values of the parameters, $a=b$, $c=\infty$ in equation (2.4), and a, $b=c=\infty$ in equation (2.5) would largely be averaged out in a real experimental situation.

The spherical symmetry of most of our functions forces us to use a spherical range of measurement. Cooper & Rouse (1968) showed, with the example of sodium chloride, that the assumption of a spherical range of measurement does not give rise to large errors in the TDS correction provided the size of the sphere is properly chosen. Lucas (1969) used the spherical approximation with potassium chloride and compared his results with Mössbauer-spectroscopic data, whereby he obtained reasonable agreement.

The use of the interference function (2.2), and the resolution functions (2.3), (2.4), and (2.5) enables us to evaluate five of the six integrations analytically, the sixth one must then be calculated numerically.

3. Convolution integrals

In order to evaluate the correction we need the actual intensity profile and the integral over the profile. The three-dimensional profile is given by

$$H(\mathbf{x}')=\int_{-\infty}^{+\infty} I_1(\mathbf{x}'-\mathbf{x})G(\mathbf{x})\mathrm{d}^3x\,, \tag{3.1a}$$

or by

$$H(\mathbf{x}')=\int_{-\infty}^{+\infty} I_1(\mathbf{x})G(\mathbf{x}'-\mathbf{x})\mathrm{d}^3x\,. \tag{3.1b}$$

cf. Hosemann & Bagchi (1962, p. 72), Als-Nielsen & Dietrich (1967) and Cochran (1969). The integral of the profile over the range of measurement is then

$$\alpha_R=\int_v H(\mathbf{x}')\mathrm{d}^3x'=\langle H(\mathbf{x}')\rangle V, \tag{3.2}$$

where the subscript R emphasizes the fact that we have taken into account limited experimental resolution. V is the volume of the range of measurement and the brackets $\langle\ \rangle$ indicate the average taken over this range. By analogy with equation (3.2) we obtain for the background

$$\alpha'_R=\ll H(\mathbf{x}')\gg V, \tag{3.3}$$

where the double brackets indicate the average taken over the area of background measurement [*cf.* Cochran, 1969, equation (3.9)]. The TDS correction, expressed in terms of the observed and corrected structure factors, may then be written as

$$|F_{obs}|^2=|F_{corr}|^2(1+\alpha_R-\alpha'_R)\,. \tag{3.4}$$

Let $\alpha-\alpha'$ be the correction which is obtained solely with the interference function, then the factor

$$R=\frac{\alpha_R-\alpha'_R}{\alpha-\alpha'} \tag{3.5}$$

formally describes the effect of limited experimental resolution on the correction $\alpha-\alpha'$. Since the effect of limited resolution is to flatten the profile, one would expect that

$$\alpha_R\leq\alpha\,,\quad \alpha'_R\geq\alpha'\,,\quad R\leq 1\,.$$

So far the equations in this section have been kept completely general in order to lay out the essential

features of our problem concisely. In order to be able to evaluate the integrals we now have to choose expedient coordinates. Because of the spherical symmetry of our interference function (2.2) we introduce polar coordinates. $\mathbf{x} \rightarrow \theta$, φ, r, and $\mathbf{x}' \rightarrow \theta'$, φ', ϱ. Using equations (2.2), (2.3), and (3.1*a*) we obtain for the profile

$$H(\theta'\varphi'\varrho) = C\left(\frac{a}{\pi}\right)^{3/2} \times \int_{r=0}^{\infty}\int_{\theta=0}^{\pi}\int_{\varphi=0}^{2\pi} \exp(-ar^2) r^2 \sin\theta \,\mathrm{d}\theta\,\mathrm{d}\varphi\,\mathrm{d}r \times [N_1^{-2} + \varrho^2 + r^2 - 2r\varrho(\sin\theta\cos\varphi\sin\theta'\cos\varphi' + \sin\theta\sin\varphi\sin\theta'\sin\varphi' + \cos\theta\cos\theta')]^{-1}. \quad (3.6)$$

A corresponding approach using equation (3.1*b*) instead of (3.1*a*) would also be possible and is proposed by Hosemann & Bagchi (1962, p. 69) for the calculation of profiles. Further investigation shows, however, that with the use of equation (3.1*b*) only four of the six integrals involved in equation (3.2) can be evaluated analytically. Therefore we have to drop this type of approach. For a spherical range of measurement with radius $\varrho = \gamma$, and volume $V = (\frac{4}{3})\pi\gamma^3$ we now obtain

$$\alpha_R = \int_{\varrho=0}^{\gamma}\int_{\theta'=0}^{\pi}\int_{\varphi'=0}^{2\pi} H(\theta'\varphi'\varrho)\varrho^2 \sin\theta' \,\mathrm{d}\theta'\,\mathrm{d}\varphi'\,\mathrm{d}\varrho\,. \quad (3.7)$$

The integrations which occur in equations (3.6) and (3.7) are carried out in the Appendix. Here we present the results of five integrations for α_R, and of two integrations for the profile. Using the three-dimensional resolution function (2.3) we obtain

$$\alpha_{R3} = C4\pi\left(\frac{a}{\pi}\right)^{3/2}\int_{r=0}^{\infty} \exp(-ar^2) r^2 D(r,\gamma)\,\mathrm{d}r\,, \quad (3.8)$$

where $D(r,\gamma)$ is defined in equation (*A*4). For the profile we obtain

$$H(\varrho) = C\frac{\pi}{\varrho}\left(\frac{a}{\pi}\right)^{3/2}\int_{r=0}^{\infty} \exp(-ar^2) r \times \ln\left[\frac{(\varrho+r)^2 + N_1^{-2}}{(\varrho-r)^2 + N_1^{-2}}\right]\mathrm{d}r\,. \quad (3.9)$$

Because of the spherical symmetry of I_1 and G the profile does not depend on θ' and φ'.

For the two and one-dimensional resolution functions we determine α_R and the profiles by choosing suitable coordinates of integration. In the two-dimensional case the instrumental broadening may extend in the xy plane. This is the plane of the angle φ, while $\theta = 90°$. Using the two-dimensional resolution function (2.4) we obtain

$$\alpha_{R2} = C2a\int_{r=0}^{\infty} \exp(-ar^2) r D(r,\gamma)\,\mathrm{d}r\,, \quad (3.10)$$

$$H(\theta'\varrho) = C\frac{4a}{\pi}\int_{r=0}^{\infty} \exp(-ar^2) r \arccos(D_1/D_2)\,\mathrm{d}r \times (D_2^2 - D_1^2)^{-1/2}, \quad (3.11)$$

where

$$D_1 = -2\varrho r\sin\theta'\,, \quad D_2 = N_1^{-2} + \varrho^2 + r^2.$$

In the one-dimensional case the instrumental broadening may extend in the **z** direction, then $\theta = 0°$ and $\theta = 180°$ for the positive and negative **z** directions respectively. φ is not relevant. Using the one-dimensional resolution function (2.5) we obtain

$$\alpha_{R1} = C2\left(\frac{a}{\pi}\right)^{1/2}\int_{r=0}^{\infty} \exp(-ar^2) D(r,\gamma)\,\mathrm{d}r\,, \quad (3.12)$$

$$H(\theta'\varrho) = C\left(\frac{a}{\pi}\right)^{1/2}\int_{r=-\infty}^{r=+\infty} \exp(-ar^2)\,\mathrm{d}r \times [N_1^{-2} + \varrho^2 + r^2 - 2\varrho r\cos\theta']^{-1}. \quad (3.13)$$

For the background at $\varrho = \gamma$ we obtain according to equation (3.3)

$$\alpha'_R = \tfrac{4}{3}\pi\gamma^3 H(\theta'\gamma)\,. \quad (3.14)$$

We do not, however, calculate an average of the profile over a certain area of background measurement since, with the model we use, this would give rise to severe mathematical complications. But renouncing the evaluation of such an average does not really affect our results because we do not wish to simulate a particular experimental situation but only want to determine the basic trend of the effect of limited resolution.

The integrals over the variable r were calculated numerically. For this purpose a special program was written. In principle, the integrations have to be performed to the upper limit $r_{max} = \infty$. In practice this is impossible; however, it is not necessary since the factor $\exp(-ar^2)$ converges rapidly to zero. A smaller value of r_{max} should be used also for physical reasons: the convolution operation should be performed within the first Brillouin zone because the interference function (2.2) holds only within this zone. If we equate the volumes of the cube-shaped and spherical forms of the Brillouin zone, we obtain 0·620 as an effective radius of the zone. In the most unfavourable case the coordinates ϱ and r are added, hence we should fulfil the condition $\varrho + r_{max} \leq 0{\cdot}620$. The largest value of ϱ is γ, the radius of the range of measurement. With $r_{max} = 3\gamma$ the integrals were already properly computed as could be checked by comparison with larger values of r_{max}. Thus with $r_{max} = 3\gamma$ and $\varrho_{max} = \gamma$ the numerical integration is restricted to apply to the case $4\gamma \leq 0{\cdot}620$, or $\gamma \leq 0{\cdot}155$. In general 200 points were sufficient to compute the integrals properly; in some cases 1000 points were needed.

4. Results

Since a mosaic block in the crystal has about 500 to 10000 cells in each direction of space, we have per-

formed the calculation with $N_1 = 10^3$ and $N_1 = 10^4$. The results are nearly the same for these two values of N_1, except for very small values of γ (range of measurement) and extremely high resolution.

The first calculations were performed in such a way that γ, the position of background calculation, was chosen so that the resolution function decreased to 10^{-3} of its maximum value, *i.e.* $\exp(-a\gamma^2) = 10^{-3}$. In this way the constant a and the resolution function is defined for each value of γ. The result of this type of calculation was that, for quite different values of γ and the corresponding resolution functions, the R factors (3.5) are nearly the same. With the three-dimensional resolution function (2.3) we obtained $R3 \simeq 0{\cdot}81$. With the two and one-dimensional functions, (2.4) and (2.5) respectively, we obtained $R2$ and $R1$ values which were smaller or larger than 0·8, depending on the value of θ', but these values were also nearly constant for all values of γ. This means that the absolute size of the range of measurement has only a minor effect on the R factor (3.5). Thus it is of primary interest to vary the resolution function with respect to a given size of the range of measurement. In order to do this we have introduced a second parameter, B, according to

$$\exp\{-a(B\gamma)^2\} = 10^{-3}. \qquad (4.1)$$

Although a second parameter is, strictly speaking, not necessary it facilitates concise numerical representation. In equation (4.1) B and γ are given set values, and thus a is determined. γ remains the position of background calculation. Values of $B < 1$ mean that the resolution function falls to 10^{-3} of its maximum value at a smaller value than γ, namely at $B\gamma$. Thus for small (large) values of B the resolution function is sharpened (broadened), *cf.* Fig. 1. In Figs. 2, 3 and 4 the R factor is represented as a function of the factor B, for three-dimensional broadening with $\gamma = 0{\cdot}01$ and $\gamma = 0{\cdot}1$, for two and one-dimensional broadening with $\gamma = 0{\cdot}1$ and four values of θ' (0, 30, 60, 90°) for which the background was calculated. 12 points of each curve were computed, $N_1 = 10^3$. The two curves $R3$ *vs.* B lie closely together. The absolute size of the range of measurement is of minor importance, as stated above. But the size of the range of measurement relative to the sharpness of the resolution function (radius of Bragg peak) has a pronounced effect on the R factor. If the background is calculated far from the Bragg peak (small values of B) then $R \simeq 1$; if it is calculated very close to the Bragg peak then $R < 1$, *i.e.* in this case instrumental broadening reduces the correction $\alpha - \alpha'$ markedly. For the two and one-dimensional resolution functions there is also a strong dependence of the R factor on the direction in which the background is calculated. If the background is calculated in a direction of instrumental broadening ($\theta' = 90°$ for $R2$, $\theta' = 0°$ for $R1$) then R attains its minimum value; if the background is calculated in a direction perpendicular to instrumental broadening then R is nearly unity, *cf.* Figs. 3 and 4. It is remarkable that $R2$ and $R1$ are smaller than $R3$ whenever the background is calculated in a direction of instrumental broadening. In actual practice these extreme situations will never be realized, but our calculation shows that even one or two-dimensional instrumental broadening can have a pronounced effect on the R factor, and thus on the correction $\alpha - \alpha'$.

Our results follow, of course, directly from the formulae in § 3, but a more illustrative explanation of them can be obtained by comparing the interference function with the actual profiles. Interference function and some profiles are shown in Figs. 5, 6, and 7; the resolution functions were calculated for $B\gamma = 0{\cdot}05$ and $B\gamma = 0{\cdot}1$; $N_1 = 10^3$. In each case the peaks of the profiles at $\varrho = 0$ are much lower than those of the interference functions. For larger values of ϱ ($\varrho > 0{\cdot}5\ B\gamma$) the profiles attain larger values than the interference function, and for very large values of ϱ the profiles approach the interference function closely. Hence, if the background is calculated far from the Bragg peak (*i.e.*

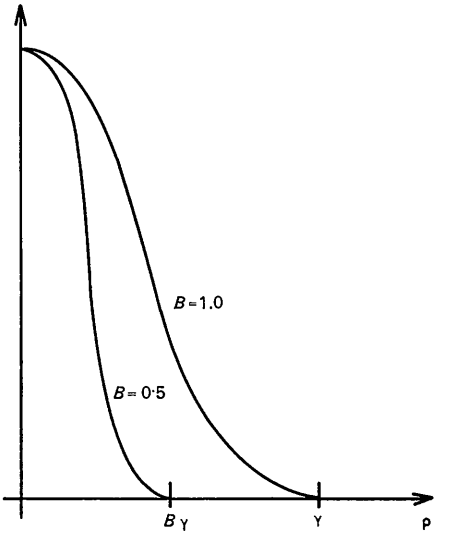

Fig. 1. Definition of the parameter B. The constant a of the resolution function is obtained for a given value of $B\gamma$ from $\exp\{-a(B\gamma)^2\} = 10^{-3}$. The background is calculated at the position γ. (The two functions shown are scaled to the same maximum value at $\varrho = 0$.)

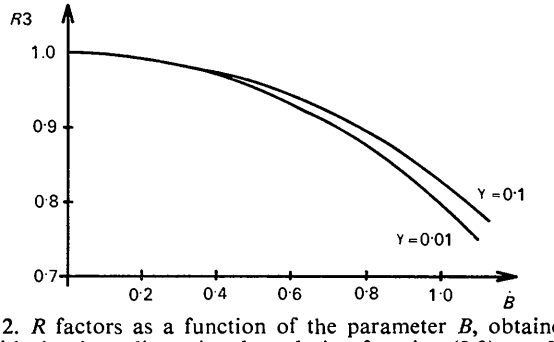

Fig. 2. R factors as a function of the parameter B, obtained with the three-dimensional resolution function (2.3); $\gamma = 0{\cdot}1$ and $\gamma = 0{\cdot}01$.

for very large values of ϱ) R approaches unity because profiles and interference function have nearly the same values, as do the respective integrals α_R and α.

A peculiarity, for one and two-dimensional broadening, is given by the profiles which run perpendicular to the directions of broadening: these profiles always have smaller values than the interference function. Thus the restriction of instrumental broadening to only one or two dimensions has the effect that the intensity

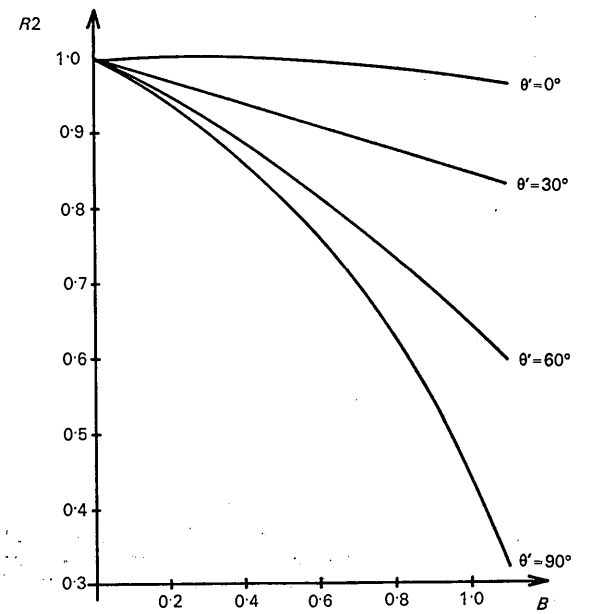

Fig. 3. R factors as a function of the parameter B, obtained with the two-dimensional resolution function (2.4); $\gamma=0{\cdot}1$. $\theta'=90°$ defines the plane of instrumental broadening ($x'y'$ plane). The background and $R2$ were calculated for $\theta'=0$, 30, 60, 90°.

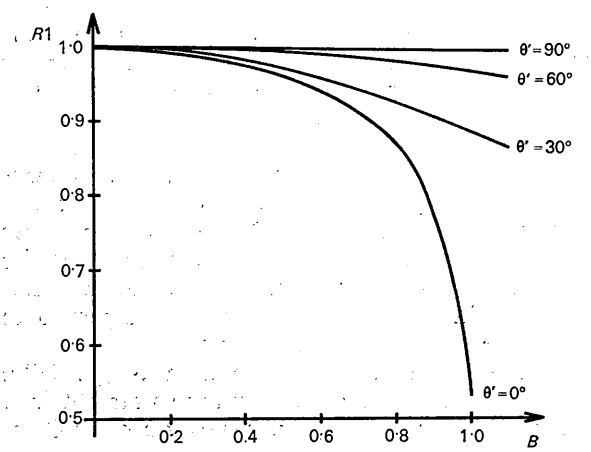

Fig. 4. R factors as a function of the parameter B, obtained with the one-dimensional resolution function (2.5); $\gamma=0{\cdot}1$. $\theta'=0°$ defines the line of instrumental broadening (z' axis). The background and $R1$ were calculated for $\theta'=0$, 30, 60, 90°.

is primarily 'pushed' into the plane or line of broadening and 'subtracted' from the space perpendicular to that plane or line respectively. This is the reason why $R2$ and $R1$ are smaller than $R3$ if the background is calculated in the plane ($\theta'=90°$) or line ($\theta'=0°$) of broadening respectively. In the case of two-dimensional broadening the 'subtraction' of the intensity from the z' direction ($\theta'=0°$) and its neighbourhood even has the effect that the intensity maximum is no longer at the centre (at $\varrho=0$) but rather along a ring around the centre ($\varrho=$constant, $\theta'=90°$) in the plane of broadening, *cf.* Fig. 6. In the one-dimensional case the intensity maximum is not observed to lie at two points $\varrho>0$ on the line of broadening, *cf.* Fig. 7. Here the intensity is subtracted from the whole plane $\theta'=90°$ and its neighbourhood so that the subtraction of intensity in the centre of the plane at $\varrho=0$ only amounts to a small part of the total subtraction.

In order to judge the effect of instrumental broadening on the TDS correction $\alpha-\alpha'$ in actual practice, one has to assess the range of the B factors that would correspond to normal experimental situations. We can do this, at least approximately, with the aid of the profiles in Fig. 5. The profile $H(\varrho)$ represents the decrease of TDS intensity, taken from a reciprocal-lattice point. The profile of the Bragg peak is not shown in Fig. 5, but we know that it has fallen to 10^{-3} of its maximum value for that value of ϱ which is given by putting $B=1$. Thus, for the two profiles drawn in Fig. 5 the Bragg peak is reduced to 10^{-3} for $\gamma=0{\cdot}1$ and $\gamma=0{\cdot}05$ respectively. As Fig. 1 shows, for $B=1$ the point γ of background calculation marks a position which lies 'beside' the Bragg peak but is still fairly close to it. For $B=1$ we may call the point γ the 'effective radius' of the Bragg peak in reciprocal space; beyond this radius the Bragg peak has only negligible intensity. (For the three-dimensional Gaussian function (2.3) 99·67% of the total intensity lies within the sphere which has the 'effective radius'.) Now, if the background is calculated at the 'effective radius' of the Bragg peak, we find from Fig. 2 that the R factor is about 0·80, and hence the overcorrection amounts to 20% of the correction $\alpha-\alpha'$. This may be considered as the upper limit likely to occur in practice. If the backgroud is calculated at twice the 'effective radius' of the Bragg peak (this corresponds to the curve with $B=0{\cdot}5$ in Fig. 1) the R factor is about 0·95, and thus the overcorrection amounts to 5% of $\alpha-\alpha'$. For three times the 'effective radius' ($B=0{\cdot}33$) we obtain an overcorrection of about 3%. Hence B values of 0·4 to 0·8, and thus overcorrections of 3 to 11% of $\alpha-\alpha'$ may be expected in normal experimental situations.

5. Conclusions

The calculations with our simple model confirm Cochran's (1969) conjecture that, due to the effectof limited instrumental resolution, the TDS correction $\alpha-\alpha'$ is generally too large. The overcorrection is considerable

if the range of measurement is small and approaches the Bragg peak closely. Then it may attain 20% or more of $\alpha-\alpha'$. In actual practice such a large value of the overcorrection will rarely be realized because the range of measurement is generally large in two directions, namely in those directions of reciprocal space which are given by the area of the detection window. It is in this area where the intensity of the background is averaged, and this area often extends, say, to twice or three times the 'effective radius' of the Bragg peak. This corresponds to $B=0{\cdot}50$ to $0{\cdot}33$, and, from our three-dimensional results, to an overcorrection of 3 to 5%. Since, in the direction of scan the background is often measured closer to the Bragg peak than twice the 'effective radius', one would expect the vercoorrection to be larger than 5% in actual cases.

There are essentially two main cases of intensity correction, and with respect to them we can draw the following conclusions.

(1) A TDS correction is not performed since, as a rule, the elastic constants of the crystal are unknown and programs for calculating the correction are not at hand. This holds for the great majority of structure determinations. In this case it is suggested that the background measurement is performed as close as possible to the Bragg peak and that the detection window is kept as small as possible. Then the correction $\alpha-\alpha'$ will already be small and the R factor notably smaller than unity, whereby the proper correction $R(\alpha-\alpha')$ will be even more reduced.

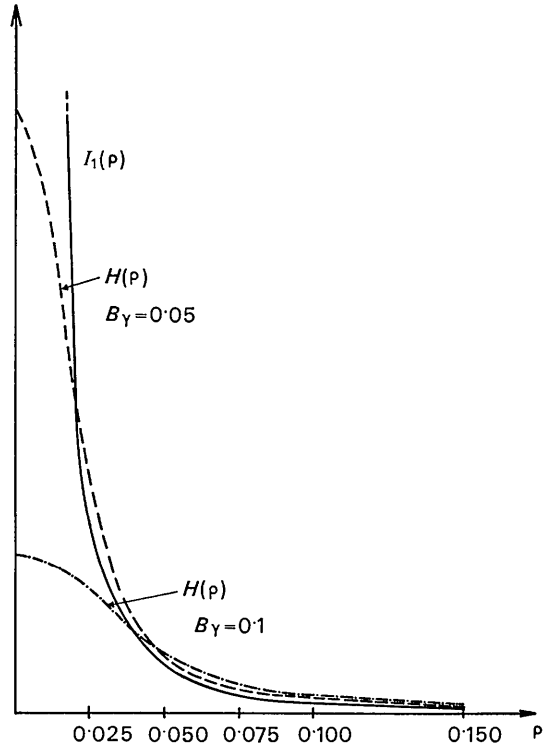

Fig. 5. Interference function $I_1(\varrho)$ and profiles $H(\varrho)$, obtained with the three-dimensional resolution function (2.3), for $B\gamma=0{\cdot}1$ and $B\gamma=0{\cdot}05$.

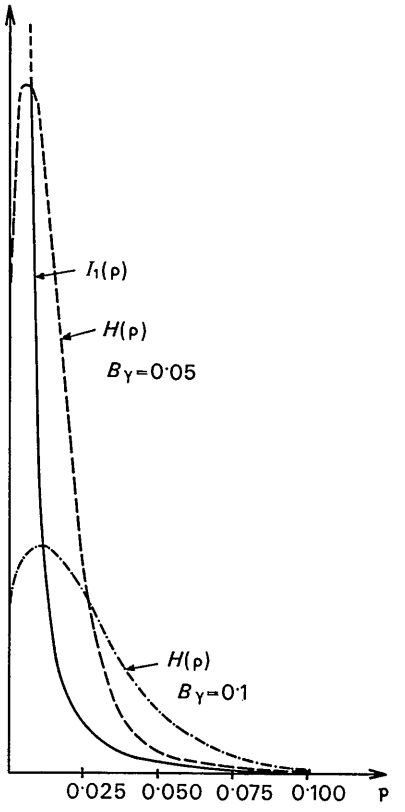

Fig. 6. Interference function $I_1(\varrho)$ and profiles $H(\varrho)$, obtained with the two-dimensional resolution function (2.4), for $B\gamma=0{\cdot}1$ and $B\gamma=0{\cdot}05$. The profiles are in the plane of instrumental broadening, $\theta'=90°$.

(2) The elastic constants are known and the TDS correction is performed. There are two cases.

(*a*) Resolution is not taken into account and only $\alpha-\alpha'$ is determined. In this case one would conclude that it is best to perform the background measurement far from the Bragg peak and to open the detection window wide. Then R will be about unity. The disadvantages of this procedure are, however, that the measurement of the peak contains an unnecessarily large amount of background, which impairs the counting statistics. Furthermore, the TDS correction becomes large in itself which gives rise to larger errors if, for some reason or other, the correction is not properly evaluated. Thus only a compromise with respect to all sources of error seems to be possible.

(*b*) Limited instrumental resolution is (partially) taken into account. The best solution so far obtained seems to be the procedure proposed by Walker & Chipman (1970) and by Jennings (1970). This procedure consists of evaluating the one-dimensional resolution function in the direction of scan and of opening the detection window so that the effects of instrumental broadening are eliminated in the other two dimensions

(area of background measurement). For a finite size of the detection window the errors of this procedure seem to lie in the range of 1 to 3% of the correction $\alpha-\alpha'$, provided that all other details of the correction are performed without any errors.

I am indebted to Mrs H. Kruse for having written most of the programs for numerical integration and for having carried out the computations on an IBM 360/65 computer. I acknowledge the discussions on thermal diffuse scattering which I have had with Professor W. Hoppe.

APPENDIX

(1) *Derivation of the profile $H(\varrho)$ and the integral α_R with the three-dimensional resolution function* (2.3)

Because of the spherical symmetry of the profile (3.6) the integrations over θ' and φ' in (3.7) result in the spherical angle 4π. Thus essentially three integrations have to be performed: over θ, φ; over r; over ϱ. There are six possible sequences for carrying them out but only one can be accepted: (1) θ, φ, (2) ϱ, (3) r. With this sequence only one integration (over r) is left to be carried out numerically; every other sequence leaves two integrals unresolved.

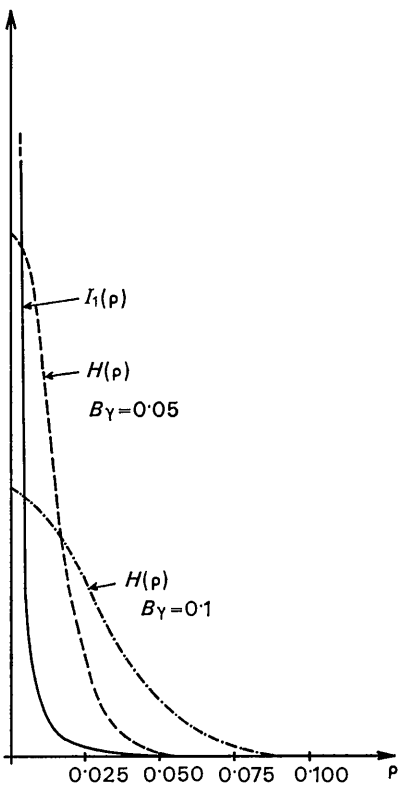

Fig. 7. Interference function $I_1(\varrho)$ and profiles $H(\varrho)$, obtained with the one-dimensional resolution function (2.5), for $B\gamma=0{\cdot}1$ and $B\gamma=0{\cdot}05$. The profiles lie along the line of instrumental broadening, $\theta'=0°$.

We begin to integrate equation (3.6) over the variables θ and φ. For this double integral a standard form exists, *cf.* Ryshik & Gradstein (1963, p. 217), and we obtain

$$H(\varrho)=C\left(\frac{a}{\pi}\right)^{3/2}\int_{r=0}^{\infty}\exp(-ar^2)r^2 \times 2\pi\int_{-1}^{+1}\frac{\mathrm{d}t\mathrm{d}r}{N_1^{-2}+\varrho^2+r^2-2\varrho rt}. \quad (A1)$$

Because of the spherical symmetry of I_1 and G the profile does not depend on the angles θ' and φ'. The integral over the variable t can be evaluated by using standard forms, and this leads to equation (3.9). In order to obtain α_R we substitute the result (3.9) in equation (3.7), write the logarithm of the ratio as the difference of the logarithms, and perform the integration over the angles θ' and φ', which gives the spherical angle 4π. Then we obtain

$$\alpha_{R3}=C4\pi\left(\frac{a}{\pi}\right)^{3/2}\int_{r=0}^{\infty}\exp(-ar^2)r^2 \times\int_{\varrho=0}^{\gamma}\pi\frac{\varrho}{r}\{\ln[(\varrho+r)^2+N_1^{-2}] -\ln[(\varrho-r)^2+N_1^{-2}]\}\mathrm{d}\varrho\mathrm{d}r. \quad (A2)$$

We abbreviate the definite integral over ϱ to $D(r,\gamma)$. In order to perform the integration over ϱ one now has to substitute $x=\varrho+r$ and $x=\varrho-r$ respectively. Then one obtains the integrals

$$\int\varrho\ln[(\varrho\pm r)^2+N_1^{-2}]\mathrm{d}\varrho =\int x(\ln x^2+N_1^{-2})\mathrm{d}x\pm r\int\ln(x^2+N_1^{-2})\mathrm{d}x. \quad (A3)$$

The two integrals can be evaluated by using standard forms *cf.* Ryshik & Gradstein (1963, p. 120) and Rottmann (1960, p. 145). If we substitute the old variable ϱ in the solutions obtained and set the limits $\varrho=0$ and $\varrho=\gamma$ we finally obtain

$$D(r,\gamma)=\pi\left\{\frac{1}{2r}(\gamma^2-r^2+N_1^{-2})\ln\left[\frac{(\gamma+r)^2+N_1^{-2}}{(\gamma-r)^2+N_1^{-2}}\right] -\frac{2}{N_1}[\arctan\{N_1(\gamma+r)\}+\arctan\{N_1(\gamma-r)\}]\right\}+2\pi\gamma. \quad (A4)$$

From equations (*A*2) and (*A*4) our result (3.8) for α_R is established. If, in the limit, we put $N_1=\infty$ then $D(r,\gamma)$ is reduced considerably. We have also derived the corresponding expression directly from equation (*A*2) which confirms our result (*A*4). For $N_1=\infty$ a singularity arises in $D(r,\gamma)$ for $r=\gamma$ which causes difficulties in the numerical integration over the variable r. Therefore we have derived equation (*A*4) for finite values of N_1.

(2) *Derivation of the profile $H(\theta'\varrho)$ and the integal α_R with the two-dimensional resolution function* (2.4)

The angle φ is in the xy plane, while $\theta=90°$. Then $z=0$, $r^2=x^2+y^2$, and the volume element of integration is $r\mathrm{d}\varphi\mathrm{d}r$. Using the two-dimensional resolution function (2.4) we obtain for the profile

$$H(\theta'\varphi'\varrho)=C\frac{a}{\pi}\int_{r=0}^{\infty}\int_{\varphi=0}^{2\pi}\exp(-ar^2)r\mathrm{d}\varphi\mathrm{d}r \qquad (A5)$$
$$\times[N_1{}^{-2}+\varrho^2+r^2-2\varrho r(\cos\varphi\sin\theta'\cos\varphi'$$
$$+\sin\varphi\sin\varphi'\sin\theta')]^{-1}.$$

Because of the symmetry of the resolution function the profile does not depend on φ', and any value of φ' is allowed. $\varphi'=0°$ and $\varphi'=90°$ are expedient since the solutions of both the resulting integrals over φ are known in the limits from 0 to $\pi/2$ (*cf.* Rottmann, 1960, p. 164). Since both these definite integrals have the same value the total integral in the limits from 0 to 2π is four times as large. Thereby the result (3.11) is established.

In order to determine α_R we have to insert the profile (*A*5) into equation (3.7). Instead of first integrating over θ, φ we can equally well begin by integrating over θ', φ'. With the second integration over ϱ we then obtain $D(r,\gamma)$. The final integration over φ gives 2π, which establishes our result (3.10) for α_{R2}. The result (3.10) can also be gained from the result (3.8) for α_{R3} by introducing a suitable parameter c in the three-dimensional resolution function and then evaluating the limit for $c\to\infty$. This establishes an independent control for equation (3.10).

(3) *Derivation of the profile $H(\theta'\varrho)$ and the integral α_R with the one-dimensional resolution function* (2.4)

The broadening may extend in the z direction, then $\theta=0°$ for the positive and $\theta=180°$ for the negative z direction. φ is not relevant. The volume element is $\mathrm{d}r$. Using the one-dimensional resolution function (2.5) we immediately obtain the profile (3.13). In order to determine α_R we have to insert the profile (3.13) into equation (3.7). $D(r,\gamma)$ is obtained as in the two-dimensional case, and it has the same value in the positive and negative z directions. Thereby equation (3.12) is established.

(4) *Remark*

In the limit for $N_1\to\infty$, $N_1{}^{-2}\to 0$, the formulae for α_R reduce to simpler ones which can also be derived independently by direct integration of the basic equations. Furthermore, it can be shown in all cases that, in the border case of ideal resolution, α_R approaches α, and the profile H approaches the interference function I_1.

References

ALS-NIELSEN, J. & DIETRICH, O. W. (1967). *Phys. Rev.* **153**, 706–710.

COCHRAN, W. (1969). *Acta Cryst.* A**25**, 95–101.

COOPER, M. J. & ROUSE, K. D. (1968). *Acta Cryst.* A**24**, 405–410.

HOSEMANN, R. & BAGCHI, S. N. (1962). *Direct Analysis of Diffraction by Matter*. Amsterdam: North Holland.

JAMES, R. W. (1948). *The Optical Principles of the Diffraction of X-rays*. London: Bell.

JENNINGS, L. D. (1970). *Acta Cryst.* A**26**, 613–622.

LUCAS, B. W. (1969). *Acta Cryst.* A**25**, 627–631.

NILSSON, N. (1957). *Ark. Fys.* **12**, 247–257.

ROTTMANN, K. (1960). *Mathematische Formelsammlung*. Mannheim: Bibliographisches Institut.

RYSHIK, J. M. & GRADSTEIN, I. S. (1963). *Summen-, Produkt- und Integraltafeln*. Berlin: VEB Deutscher Verlag der Wissenschaften.

SKELTON, E. F. & KATZ, J. L. (1969). *Acta Cryst.* A**25**, 319–329.

WALKER, C. B. & CHIPMAN, D. R. (1970). *Acta Cryst.* A**26**, 447–455.